Roll Forging

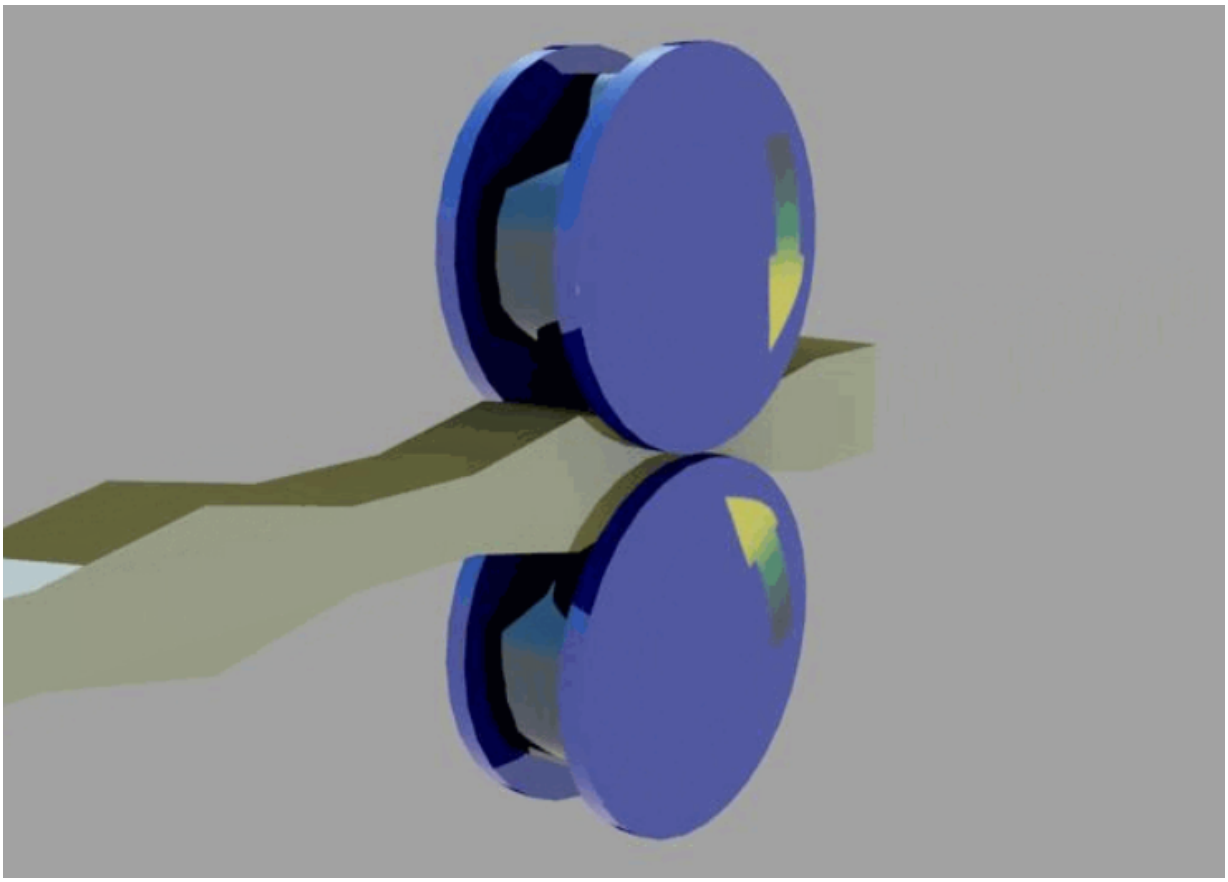

Madeline Fabela, Shawn Kuriakose, Dillan Tran, Leslie Jaramillo Martinez

Engineering Design II

Tufts University

December 16, 2021

Executive Summary

This project involved the analysis of a Roll Forging Machine - a machine that reduces cross-sectional areas while simultaneously changing the shape of heated bars. The goal of this project was to propose an effective design for the components of the roll forge and determine which component would be the first to fail. The main machine components are identified to be the bearings, rollers, and gears. Assumptions and calculations were done based on the main components, and a Finite Element Analysis (FEA) simulated by Solidworks was used to validate our results. The rollers were deemed to be the most vulnerable.

To achieve an effective design, we must use the knowledge acquired in class. The work to reach our final conclusion was a group effort and divided equally and conquered by all.

Deflection in the rollers

Load Method	Using Tables A-9	Using FEA
Point Load	3.61e-04 [m]	2.67e-04 [m]
Distributed Load	2.52e-04 [m]	1.75e-04 [m]

Tabulated Speed, Torque, and Power for gears

Gears	Speed	Torque	Power
Pinion	30 [RPM]	27.5 [kN*m]	825 [kW]
Compound	65.828 [RPM]	58.895 [kN*m]	3876.94 [kW]

Table for Safety factors

Static Failure	Fatigue Failure
4.66	1.2

Table of Contents

1 Introduction

Roll forging is a process used to pre-form a workpiece. Pre-forming is the process of redistributing the mass of the workpiece before closed die forging. The machine must be able to pre-form roll forging without generating a large volume of flash and plastic deformation. There are two types of roll forging processes: Longitudinal and Cross Roll Forging. The machine is configured for longitudinal roll forging where the workpiece passes through the rollers tangentially.

In *figure 1*, a Russian patent of a similar roll forging machine was used to make our assumptions about the process. Additionally, we were given a simplified CAD model of the machine in *figure 2*. The parts and their dimensions were used in our analysis. Furthermore, a research paper titled *Cross Wedge Rolling and Forging Rolls As Additional Devices in closed die forging* was used to make assumptions about the peak torque and peak radial loads generated and the material of components for the roll forging machine.

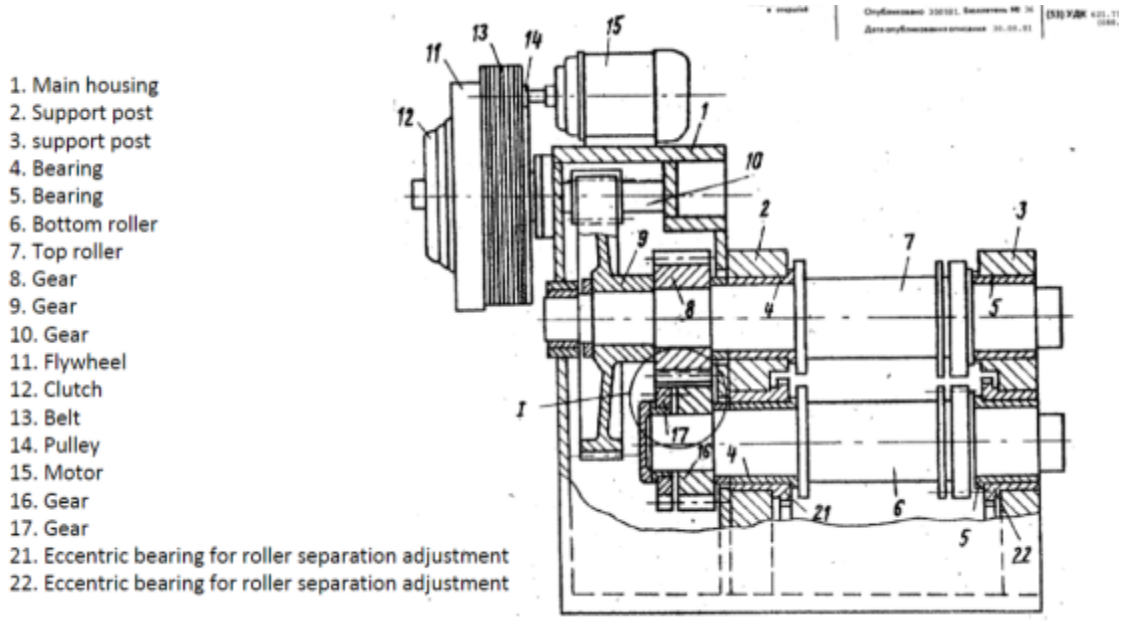

Figure 1. Patent drawing of roll forging machine with labels.

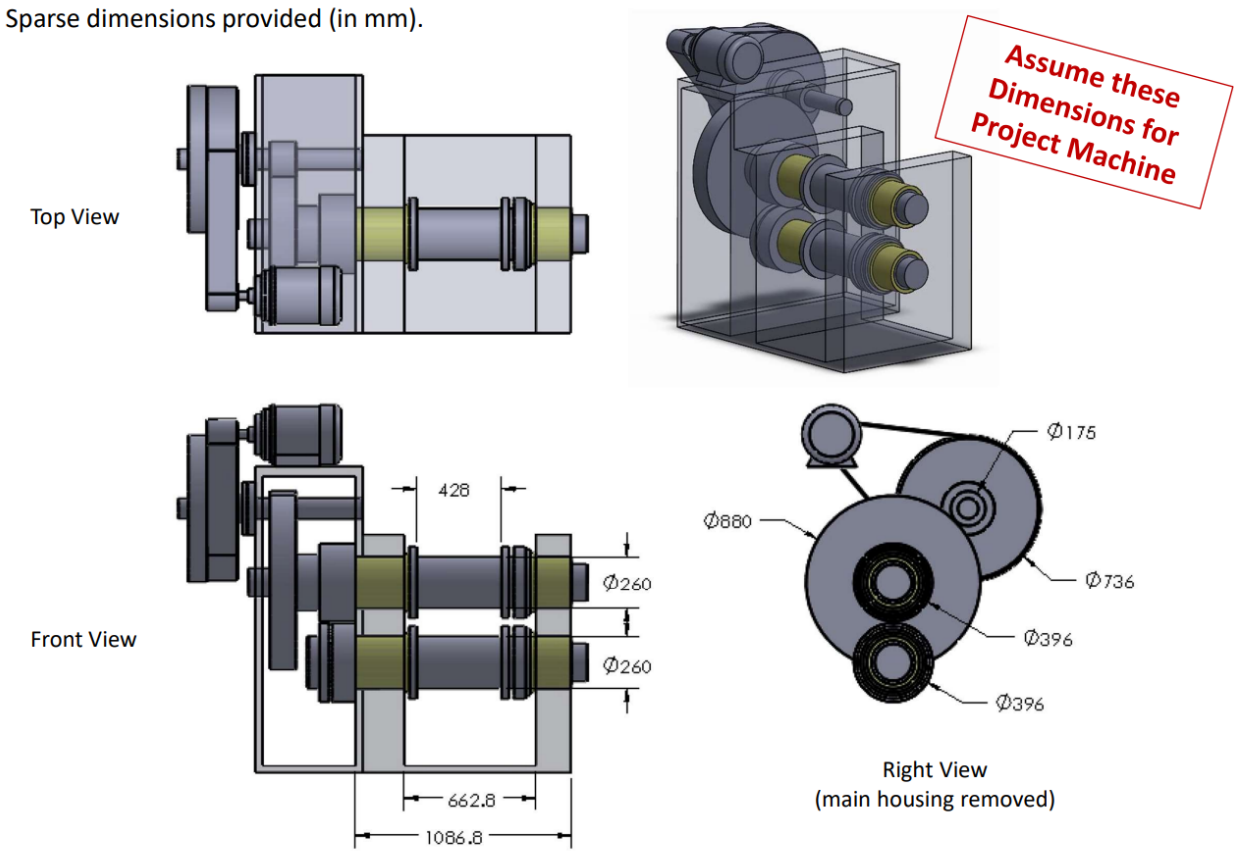

Figure 2. Simplified CAD machine design details (dimensions are in mm)

2 Roller Analysis

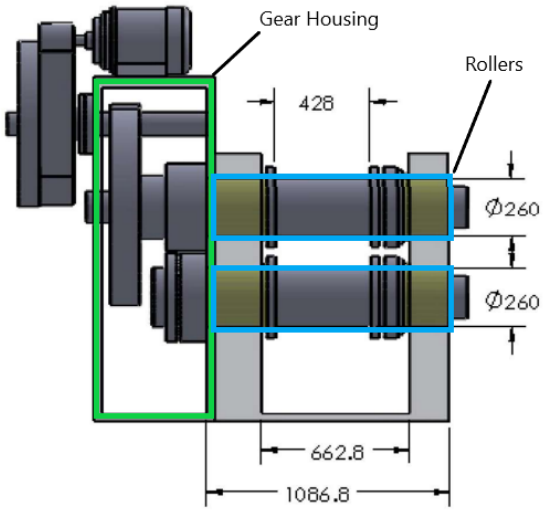

Figure 3. Front view of the machine with additional details (dimensions are in mm)

In *figure 3*, a closer look at the front of the machine is shown. Highlighted in green in the gear housing where the gears are located. The blue highlights represent the rollers of the roll forging machine, and the yellow sections at the ends of the rollers are the bearings. The rollers are fixed to the gear system and are held in place and allowed to rotate by the bearings. During operation, the rollers will face an equal and opposite force from the workpiece as it passes through. The roller can experience force from the workpiece in two different cases: as a point force or a uniformly distributed force. In the following section, both cases of deflection in the rollers are found analytically and through an FEA simulation by Solidworks. It should be noted that the analytical deflection considered the gears on the same axis of the roller to play a role in the total deflection found. On the other hand, the FEA model only considered the roller.
In the FEA Analysis, the best-case scenario was studied. The roller was fixed at opposite faces and the force was applied as a point or distributed load. This simplification was chosen to compare values. On the other hand, analytical calculations acknowledged the slight changes of total load by the gears. In reality, the gears contribute to the torque of the roller, which was not accounted for in the SolidWorks simulation.

The material chosen for the rollers was Alloy Steel SS, with properties larger than a standard material undergoing the roll forging process. The Ultimate Yield Strength, and Elastic Modulus were compared using SolidWorks material properties and MatWeb.

2.1 Analytical calculations for reaction forces at the bearings

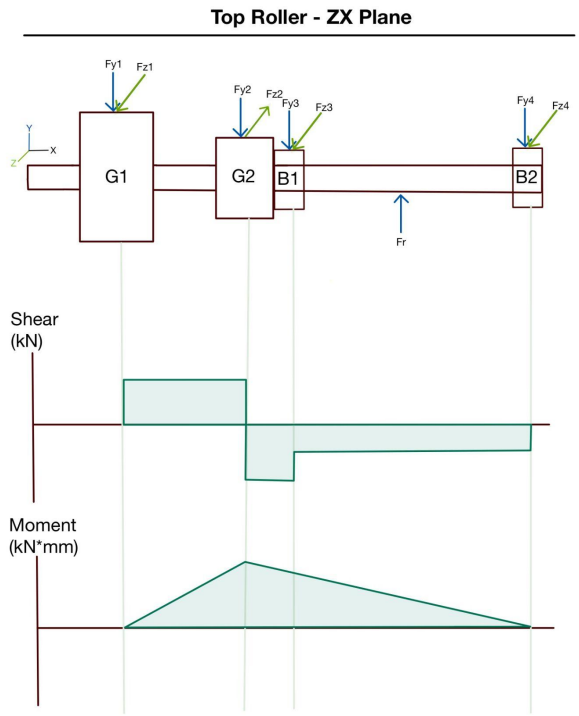

Figure 4a. Free body diagram and S-M diagrams of the top roller for forces in the Z direction. (Not scaled)

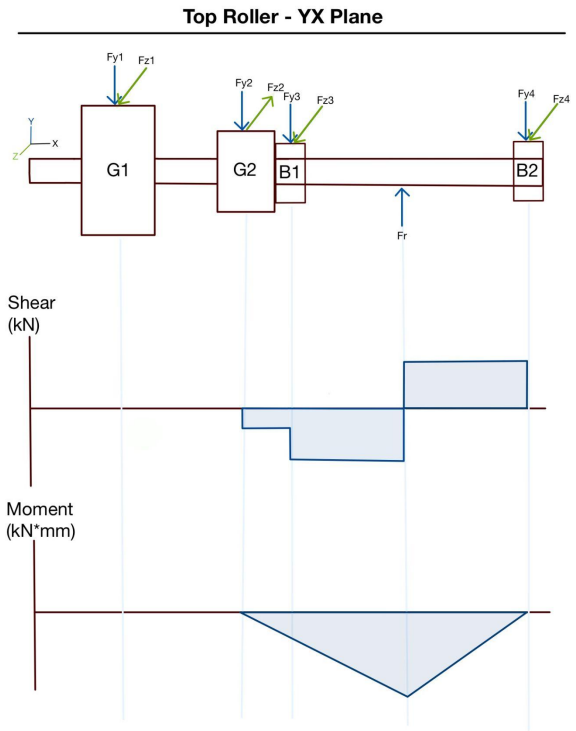

Figure 4b. Free body diagram and S-M diagrams of the top roller for forces in the Y direction. (Not scaled)

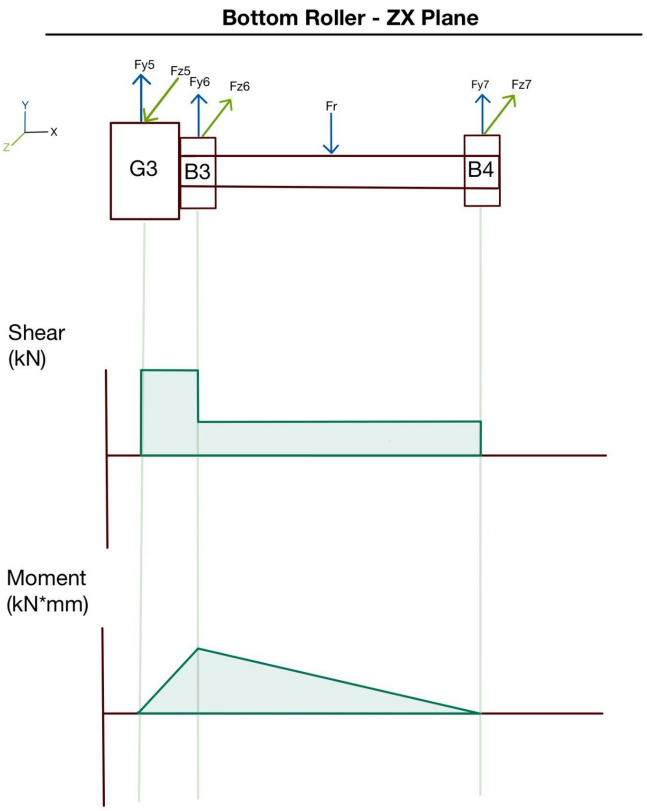

Figure 4c. Free body diagram and S-M diagrams of the bottom roller for forces in the the Z direction. (Not scaled)

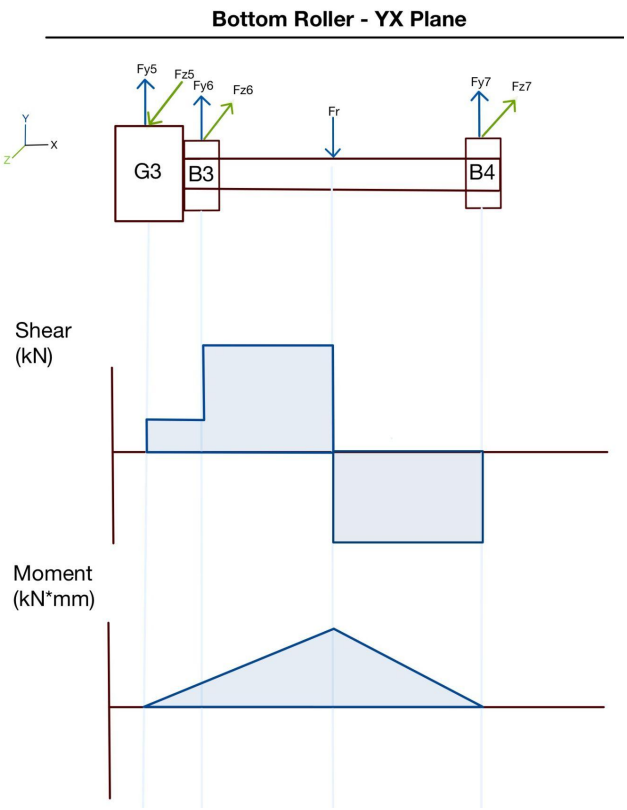

Figure 4d. Free body diagram and S-M diagrams of the bottom roller for forces in Y direction. (Not scaled)

Calculations:

Figure 4a - Forces of the top roller in the ZX plane

$$T = F_{z1}(\frac{d_1}{2})$$

$$T = F_{z2}(\frac{d_2}{2})$$

The peak torsion is 25.7 kN*m is given.

The diameter of G1 is given to be 0.88m

The diameter of G2 is given to be 0.396m

$$F_{z1} = 58.44kN$$

$F_{z2} = 129.8kN$

It is assumed that the forces at the two bearings are equal, allowing for equilibrium equations to be used for the X-Z plane.

$\Sigma F_z = 0$

$F_{z1} - F_{z2} + 2F_{z3} = 0$

$F_{z3} = F_{z4} = 35.68kN$

Figure 4b - Forces of the top roller in the XY plane

It is assumed that the Y forces on G1 are zero since the components attached to it are being ignored due to lack of knowledge of these components (the fly-wheel, pulley, motor, and G10). Now $F_{y2}$was calculated using the relationship between radial and tangential forces.

It is assumed that the pressure angle, $\alpha\ is\ 20^{\circ}$.

$F_{y2} = F_{z2}tan(\alpha)$

$F_{y2} = 23.621kN$

It is assumed that the forces at the two bearings are equal, allowing for equilibrium equations to be used for the X-Y plane.

$\Sigma F_y = 0$

$-F_{y2} + F_r - 2F_{y3} = 0$

$F_r$is the peak radial force given of 1410 kN, which was assumed to only act in the halfway point between the two bearings.

$F_{y3} = F_{y4} = 693.1895\ kN$

Figure 4c - Forces of the bottom roller in the ZX plane

$T = F_{z5}(\frac{d_1}{2})$

The peak torsion given is 25.7 kN*m.

The diameter of G3 is given to be 0.88m.

$F_{z5} = 58.44kN$

It is assumed that the forces at the two bearings are equal, allowing us to do equilibrium equations for the X-Z plane.

$\Sigma F_z = 0$

$F_{z5} + 2F_{z6} = 0$

$F_{z6} = F_{z7} = 29.20kN$

Figure 4d - Forces of the bottom roller in the XY plane

The two gears of the bottom roller are assumed to be one, G3. Since the bottom roller experiences the same forces in the Y-direction as the top roller, no further calculations are needed.

$F_{y5} = F_{y2} = 23.621kN$

$F_{y6} = F_{y3} = 693.1895\ kN$

F_r = Peak Radial = $1410\ kN$

$F_{y7} = F_{y4} = 693.1895\ kN$

It is evident that the forces in the Y-direction are the highest, meaning they are the ones that can cause the most damage. Therefore, it was decided to focus on the X-Y plane in order to proceed with the analysis. From here, an approximation of the moment diagrams were drawn, using the dimensions provided. Again, since the forces in the Y-direction are the same magnitude but opposite directions for the top and bottom roller, we can use a one moment diagram to determine the peak moment.

It is noted that the results obtained for moment are not ones that allow us to obtain a perfect moment diagram, however, this is reasonable because of all the assumptions that have been made. Additionally, it has the general shape one would expect given most of the forces act on the bearings which are the same distance apart from the peak radial force. Based on this work cohesively and that observed through the presentations other groups in the class gave, it is concluded this was a correct approach.

Figure 4b - Moments of the top roller in the XY plane

Moment acting on G1 is 0, due to there being no forces in the Y direction here.

Moment acting on G2 = $F_{y2}102mm = 2409.24$ kN*mm

Moment acting on B1 = $(F_{y2} + F_{y3})\frac{662.8mm}{2} = 237{,}551$ kN*mm

Moment acting on B2 = $F_r - (F_{y2} + F_{y3})\frac{662.8mm}{2} = 229{,}723$ kN*mm

Again, these moment calculations do not result in a perfect moment diagram, however, it is believed such fault is not significant, as many other groups assumed the moment diagrams to be that of just the bearings. These are reasonable assumptions and the calculations have proved that forces related to gears are not significant in comparison to forces on the roller and on bearings.

2.2 Two Case Analysis for deflection

Introduction

In order to estimate the deflection of the roller at the bearing locations, superposition was used. Realistically, the bearing experiences a radial load in the region where the bearing is located. Using table A-9, a reaction force at the outer ends of the bearing was used to calculate the deflection halfway the length of the bearing. Similarly, a reaction force at the center of the bearing length was used to calculate the deflection of the remaining length. Both point-load (worst-case scenario) and distributed load were calculated. These values were then compared to the deflection found using a SolidWorks simulation. In both approaches, analytical and simulation, the deflection was found to have a magnitude of -4. The deflection was not a major concern in the design of the Roll Forging Machine.

Tables A-9

Properties:

$r = 0.16\,m$

$l = 1.0868\,m$

$S_{UT} = 723.826\,MPa$

$S_y = 620\,MPa$

$$E = 210,000\ MPa$$

$$I = \frac{\Pi d^4}{64} = \frac{\Pi(0.26)^4}{64} = 2.243 \cdot 10^{-4}\ \frac{kg}{m^2}$$

Point load:

To calculate total deflection at the bearing location, assuming that the reaction force behaves radially, a further simplification was necessary. The deflection halfway across the bearing location was calculated using a reaction force acting at the extreme outer edges, and a second calculation was done at the center of the bearing. Realistically, the reaction force would be distributed across the entire length. Assuming point reaction forces at the two locations chosen would also be a worst-case scenario.

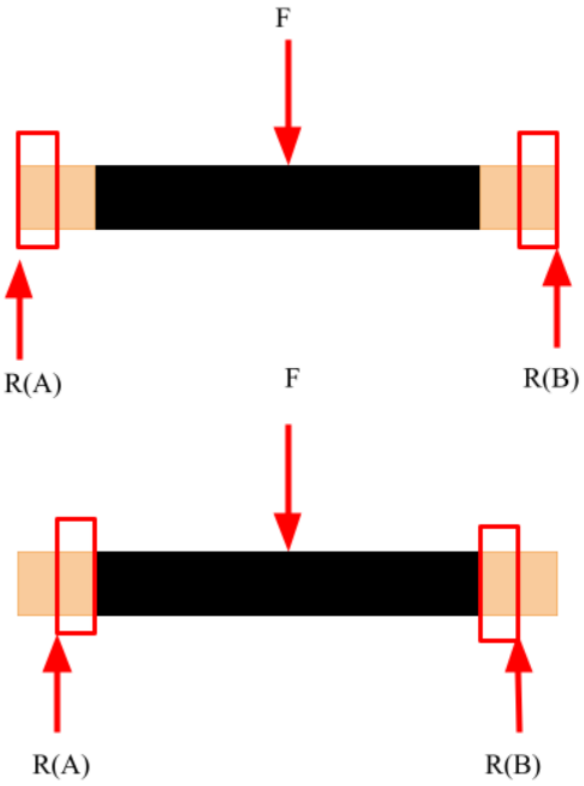

$$R_A = R_B = \frac{F}{2} = \frac{1.41\ [MN]}{2} = 705\ kN$$

$$y_{AB} = \frac{Fx}{48EI}(4x^2 - 3l^2)$$

$$\theta_{AB} = \frac{dy}{dx} = \frac{F}{EI}\left(\frac{x^2}{4} - \frac{l^2}{16}\right)$$

$$y_1 = \frac{1.41\cdot10^6 x}{48(2.1\cdot10^{11})(2.24\cdot10^{-4})}\left[4x^2 - 3(1.0868)^2\right] = \frac{1.41\cdot10^6(.106)}{48(2.1\cdot10^{11})(2.24\cdot10^{-4})}\left[4(.106)^2 - 3(1.0868)^2\right]$$

$$y_1 = -2.31 \cdot 10^{-4} m$$

$$\theta_1 = -.002044\ radians$$

$$y_2 = \frac{1.41\cdot10^6 x}{48(2.1\cdot10^{11})(2.24\cdot10^{-4})}\left[4x^2 - 3(.8748)^2\right] = \frac{1.41\cdot10^6(.106)}{48(2.1\cdot10^{11})(2.24\cdot10^{-4})}\left[4(.106)^2 - 3(.8748)^2\right]$$

$$y_2 = -1.298 \cdot 10^{-4} m$$

$$\theta_2 = -.001265\ radians$$

$$y_{total} = y_1 + y_2 = \quad -3.6078 \cdot 10^{-4} m$$

$$\theta_{total} = \theta_1 + \theta_2 = -.002477\ radians$$

Distributed load:

As was done with a point load above, the deflection at the bearings was calculated assuming that the reaction forces act at the far edge of the bearing and at the center.

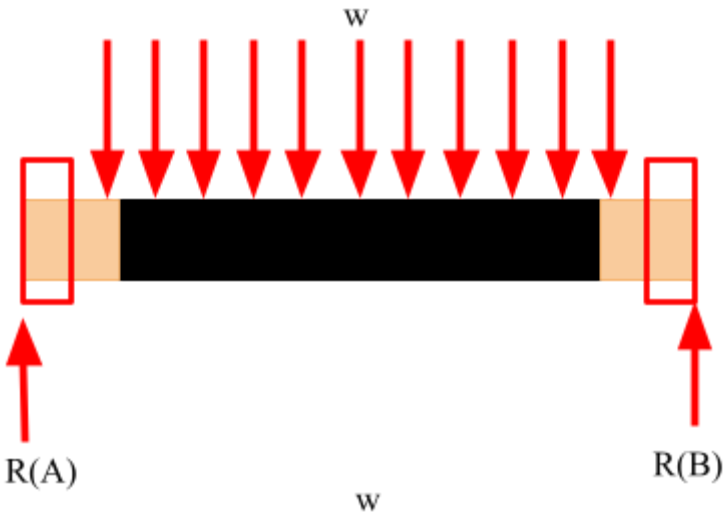

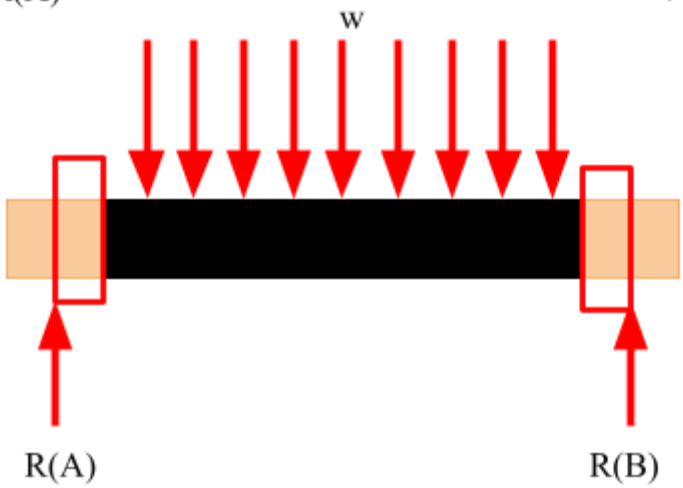

$$R_A = R_B = \frac{wl}{2} = \frac{1.41 \cdot 10^6 (1.0868)}{2} = 766194\ N$$

$$y_{AB} = \frac{wx}{24EI}(2lx^2 - x^3 - l^3)$$

$$\theta_{AB} = \frac{dy}{dx} = \frac{w}{24EI}(6lx^2 - 4x^3 - l^3)$$

$$y_1 = \frac{1.41 \cdot 10^6 (.106)}{24(2.1 \cdot 10^{11})(2.24 \cdot 10^{-4})}(2(1.0868)(.106)^2 - (.106)^3 - (1.0868)^3)$$

$$y_1 = -1.66 \cdot 10^{-4} m$$

$$\theta_1 = -.001517\ radians$$

$$y_2 = \frac{1.41 \cdot 10^6 (.106)}{24(2.1 \cdot 10^{11})(2.24 \cdot 10^{-4})}(2(.8748)(.106)^2 - (.106)^3 - (.8748)^3)$$

$$y_2 = \quad -8.606 \cdot 10^{-5} m$$

$$\theta_2 = -7.68 \cdot 10^{-4}\ radians$$

$$y_{total} = y_1 + y_2 = \quad -2.521 \cdot 10^{-4} m$$

$$\theta_{total} = \theta_1 + \theta_2 = -.001217\ radians$$

Ranges (y is positive downward):

2.521e-04 [m]< total deflection< 3.608e-04 [m]

.001717 [radians]<total slope<.00247 [radians]

SolidWorks

A simple Alloy Steel (SS) cylinder was created on SolidWorks to mimic the roller in the Roll Forge Machine. Two scenarios, a worst-case scenario in which the force was applied to a single point, and a best-case in which the force was evenly distributed. In both cases, it was assumed that the roller was fixed at opposite ends and that the only causes of deflection were the applied force and a slight deflect due to reaction forces. Due to symmetry in geometry and values of forces applied, it was assumed that both regions in which a roller bearing would be placed would experience the same deflection. Neither of the cases yielded, but there was significantly more stress with a point load in the point over which the force was applied, which would of course be a worst-case scenario.

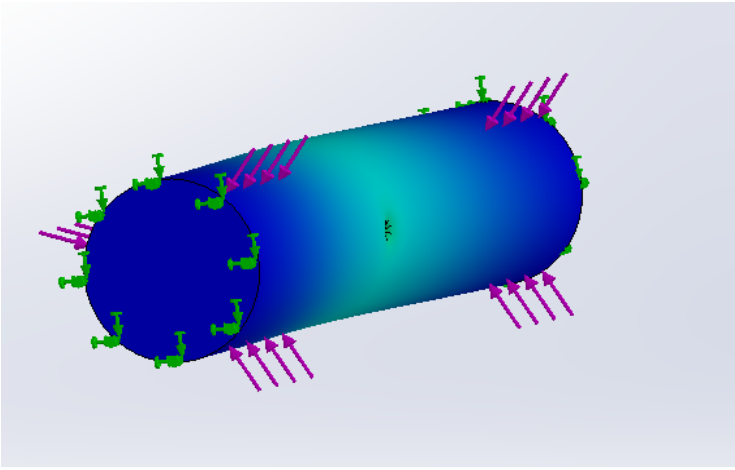

Figure 5. Simulation of a roller with an applied point load.

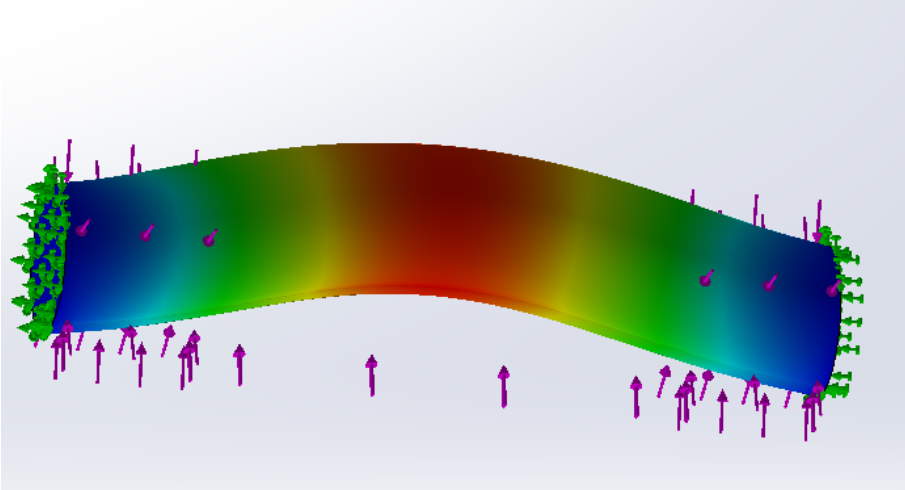

Figure 6. Simulation of a roller with a distributed load.

1.75e-04 [m]< total deflection< 2.67e-04 [m]

2.3 Roller Static and Fatigue Failure

Introduction

Of all the roll forging machine components, the rollers were put through the most extreme loading conditions and thus most likely to fail. To evaluate the roller's potential for failure, the first step was identifying the loads that the roller would experience during the longitudinal rolling process. The key loading conditions for the rollers are the normal stress in bending and shear stress in torsion on the end where the gears are located. The normal stress in bending was selected due to the peak moment on the roller that was generated by the gears to rotate both rollers. The shear stress in torsion was selected given the torsion on the roller generated by the gears and thus expected to be significant.

Choosing the instant when the system is at equilibrium, the max moments and torsions were determined using the V-M diagrams we generated based on our FBD diagram of the system.

Static Failure

Having described the FBD diagram analysis of the system, we can now determine a factor of safety guarding against static failure. Through FEA, the center of the rollers was

determined to be the location of most stress, because that is where the material that is being rolled forged is pushed through. The bending moment is maxed at the center of the roller base on the VM diagram for the XY plane. The bending moment at this location is a serious concern as this is the location where the bending moment is maximized. Using this reasoning, a stress element was selected for failure analysis at the center of the roller.

Figure 7. Location of stress element

As mentioned earlier, the primary loading conditions that are evaluated for the rollers are the normal stress in bending and the shear stress in torsion. The moment used for calculating the maximum bending normal stress is the max moment that is generated for each pass. The torsion used to calculate the torsional stress is being assumed as the max torque being generated during each pass for the performance.

$$\sigma_{bending} = \frac{Mc}{I} = \frac{(229{,}660kN)(32 * 10^3)}{\pi(260mm)^3} = 133.1\ MPa$$

$$\tau_{torsion} = \frac{Tr}{J} = \frac{(25.7kN*m)(.26/2)m*10^3}{(\Pi(.26^2)/32)} = 7.45\ \text{MPa}$$

Based on the calculation, the torsional stress appears to be negligible since it is significantly smaller than the bending stress magnitude. This result is surprising given that it's the peak torque of the gears exerted on the rollers that give the force to create the preform. For

the critical stress element, normal stress is what is causing compression of the element along the axis of the rollers while torsional stress is what causes the twisting of the element along with the rotation of the rollers.

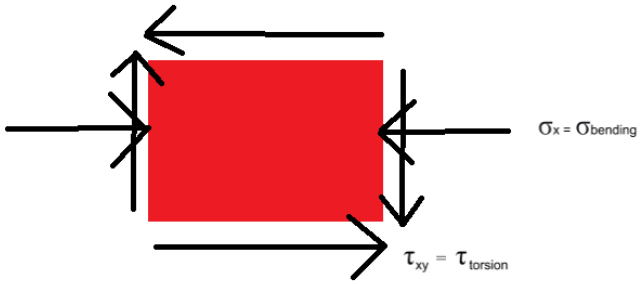

Figure 7a. labeled critical stress element

Using Distortion- Energy theory, a factor of safety guarding against static failure can be determined by employing Langer's First Cycle Yield criteria and the Von Mises stress criteria. Already assumed material choice in the FEA section.

$$\sigma'_{max} = (\sigma^2_x - \sigma_X\sigma_y + 3\tau^2_{xy})^{1/2} = ((133.09)^2 - (0) + (3)(7.45)^2)^{1/2} = 133.7\,MPa$$

$$\eta = \frac{S_y}{\sigma'_{max}} = \frac{620\,MPa}{133.7\,MPa} = 4.66$$

The factor of safety computed is greater than 1, indicating that no yielding occurs at this element of the roller. This may not be the case and in a real-life instance, could lead to instant failure of the machine entirely. What likely would have happened is that the model described was not a good representation of the roll forging machine.

Fatigue Failure

Since the safety factor for static failure is significantly greater than 1, it would be wise to check if failure is due to fatigue for the rollers. The roll forging machine is expected to operate over the course of many years for multiple hours a day. The stresses for the rollers make them

susceptible to fatigue failure over time. To determine a factor of safety guarding against failure due to fatigue we used the Stress Life Method.

When obtaining alternating stress, σ'_a , for the Goodman Approach, we are able to have τ_a be zero given the nature of the motion of the Hot Roller. Additionally, we are able to have σ_m be zero when calculating mean stress σ'_m . Lastly, when finding the maximum stress,σ'_{max}, we were able to set both, τ_a and σ_m as zero.

$$\sigma_{a,bending} = \frac{Mc}{I} = \frac{(229{,}660kN)(32 * 10^3)}{\pi(260mm)^3} = 133.1\ MPa$$

$$\sigma_{m,bending} = \frac{Mc}{I} = 0$$

$$\tau_{a,\,torsion} = \frac{Tr}{J} = 0$$

$$\tau_{m,\,torsion} = \frac{Tr}{J} = \frac{(25.7kN*m)(.26/2)m*10^3}{(\Pi(.26^2)/32)} = 7.45\ MPa$$

The expressions above can be rewritten to find the max alternating and max midplane stresses using the Von Mises Criteria similar to finding static failure.

$$\sigma'_m = ((\sigma_{m,bending})^2 + 3\,(\tau_{m,\,torsion})^2)^{1/2} = ((0)^2 + 3\,(\tau_{m,\,torsion})^2)^{1/2} = 12.9 \text{ MPa}$$

$$\sigma'_a = ((\sigma_{a,bending})^2 + 3\,(\tau_{a,\,torsion})^2)^{1/2} = ((\sigma_{a,bending})^2 + 3\,(0)^2)^{1/2} = 133\ MPa$$

Similar to what was seen in the static failure analysis, the shear stress in torsion is negligible compared to the normal stress in bending. The assumptions were made that the roll forging machine was expected to run for a total cycle time of 10 seconds, for 8 hours each day for 260 days each year at a rate of 30 RPM. These assumptions can be used to calculate the number of stress cycles.

$$N = 0.5\,rev/s * 10\,s/preform * 360\,preforms/1h * 8h/d * 260d/years * 10\,years$$

$= 3.744 * 10^6 > 10^6$

Since the number of cycles is greater than 1 million cycles used to determine the endurance stress limit, the endurance limit is then used to calculate the factor of safety guarding against fatigue failure. The endurance limit of the roller is calculated using the Stress-Life approach, which determines the endurance limit based on empirical data from R.R. Moore tests, constant amplitude load tests of carefully controlled tested specimens. The theory is employed using the help of expressions provided in *Shigley's Mechanical Engineering Design* textbook. Using the ultimate tensile strength of the roller material, the endurance limit can be estimated using expressions 6-8 from Shigley's.

$$S_e^{'} = 0.5\, S_{ut} = 361.913\ MPa\ since\ 723.826\ MPa <= 1400\ MPa$$

Since the roller setup differs from the R.R.Moore Tests, corrections have to be made to the endurance limit to account for the differences. We use Marin factors to account for these differences. Using Shigley's, five main factors are considered: surface factor, size factor, load factor, temperature factor, and reliability factor.

Given the geometry of the roller and the process that is performed, it is likely that the roller was machined. A surface factor can then be calculated using Table 6-2 from Shigley's.

$$k_a = 4.51 S_{ut}^{-.265} = .79$$

To account for the diameter of the roller loaded under the combined loading condition, expression 6-20 from Shigley's is used to calculate the size factor. For this, it is assumed that diameter is always very close to 10in, however, always smaller.

$$k_b = .91 d^{-.157} = .63$$

The roller is loaded in bending and torsion, so the load factor would simply be k_c = 1 and thus is not significant in the analysis.

The machine is expected to operate at temperatures greater than what is shown in the table for temperature factors from Shigleys. The textbook says that if that's the cause, the temperature factor can be assumed to be $k_d = 1$.

To ensure that the rollers have a reliability of 90%, a reliability factor of $k_e = .897$ is taken from Table 6-5 of Shigley's.

Using all these Marin factors, the endurance limit can be corrected.

$$S_e = k_a\, k_b\, k_c\, k_d\, k_e\, S'_e = (.79)(.63)(1)(1)(.897)(361.913\ MPa) = 161.6 \text{ MPa}$$

Now to calculate the safety factor guarding against fatigue failure, the conservative Goodman Line method was used.

$$\eta = \frac{1}{\sigma'_m/S_{ut} + \sigma'_a/S_e} = 1.2$$

The factor of safety is much less than that for static failure, and using the load lines we determined that fatigue is the failure mode.

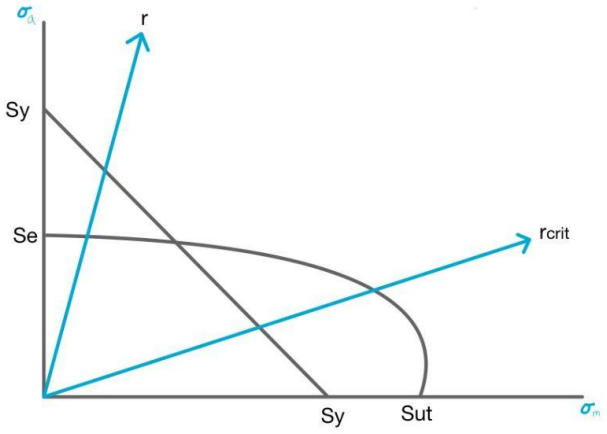

Figure 8. Plot showing $r > r_{crit}$

3 Bearing Selection

Introduction

In selecting an appropriate bearing, the elements that compose a rolling bearing must be studied: elements must fit into a specified dimension; they must be able to receive a given load, and they must satisfy operation under specified conditions. For this design, the fatigue loading, and material properties were studied. Thus, the chosen bearing did not take into consideration corrosion resistance, lubrication, or cost.

The analysis of reaction forces at the bearings concluded that pure radial load was experienced. Therefore, the bearing selection was narrowed to N and NU-type cylindrical roller bearings (SKF). At a constant load, the life measure distribution of roller bearings is right-skewed. In order to calculate the catalog life, which was used to determine an appropriate bearing type, the Weibull Distribution was used. Shafts generally have two bearings and often these bearings are different. However, in this design, it was assumed that both bearings in each roller were identical for simplification purposes. *Figure 9b* shows a range of possible bearing options from a manufacturer.

Proper lubrication, maintenance, and reasonable operating temperatures would act as mitigating factors for a bearing's failure. These properties were not included in the bearing selection but would serve as an additional effort to reduce cycles until metal fatigue.

$$C_{10} = a_f F_D \left[\frac{x_D}{x_0 + (\theta - x_0)[ln(1/R_D)]^{1/b}}\right]^{1/a}$$

$$x_D = \frac{L_D}{L_{10}} = \frac{(2080)(30)(60)}{10^6} = 3.744$$

Since we are assuming a rating life of 10^6 revolutions, Weibull Parameters were compared to those given in Table 11-6 in *Shigley's Mechanical Engineering Design (*Budynas, p.63 *)*.

Manufacturer	Rating Life, Revolutions	Weibull Parameters Rating Lives		
		x_0	θ	b
1	$90(10^6)$	0	4.48	1.5
2	$1(10^6)$	0.02	4.459	1.483

Figure 9a. Rating life and Weibull Parameters

$$C_{10} = a_f F_D \left[\frac{x_D}{x_0+(\theta-x_0)[ln(1/R_D)]^{1/b}}\right]^{1/a} = 1.2(705\ [kN])[$$

$$\frac{3.744}{0.02+4.439(ln(1/0.9))^{1/1.483}}]^{3/10} = 1317kN$$

Single row
Standard and SKF Explorer
Series: 202 EC – 244 EC
Size: 15 mm – 220 mm
0.5906 in – 8.6614 in

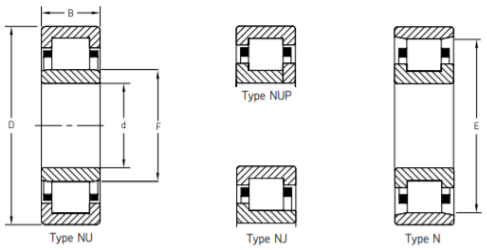

Figure 9b. SKF bearings

Designation	Principal dimensions						Basic load ratings				Speed rating		Mass		Diameter			
	Bore d		Outside diameter D		Height H		Dynamic C		Static C_0		Refer-ence speed	Limiting speed			Under roller F		Over roller E	
	mm	in	mm	in	mm	in	N	lbf	N	lbf	r/min	r/min	kg	lb	mm	in	mm	in
202 EC	15	0.5906	35	1.3780	11	0.4331	12 500	2 810	10 200	2 290	22 000	26 000	0.0	0.1	19.3	0.76	30.3	1.19
203 EC	17	0.6693	40	1.5748	12	0.4724	20 000	4 490	14 300	3 210	20 000	22 000	0.1	0.1	22.1	0.87	35.1	1.38
204 EC	20	0.7874	47	1.8504	14	0.5512	28 500	6 400	22 000	4 940	17 000	19 000	0.1	0.2	26.5	1.04	41.5	1.63
205 EC	25	0.9843	52	2.0472	15	0.5906	32 500	7 300	27 000	6 070	15 000	16 000	0.1	0.3	31.5	1.24	46.5	1.83
206 EC	30	1.1811	62	2.4409	16	0.6299	44 000	9 890	36 500	8 200	13 000	14 000	0.2	0.4	37.5	1.48	55.5	2.19
207 EC	35	1.3780	72	2.8346	17	0.6693	56 000	12 580	48 000	10 790	11 000	12 000	0.3	0.6	44.0	1.73	64.0	2.52
208 EC	40	1.5748	80	3.1496	18	0.7087	62 000	13 930	53 000	11 910	9 500	11 000	0.4	0.8	49.5	1.95	71.5	2.81
209 EC	45	1.7717	85	3.3465	19	0.7480	69 500	15 620	64 000	14 380	9 000	9 500	0.4	0.9	54.5	2.15	76.5	3.01
210 EC	50	1.9685	90	3.5433	20	0.7874	73 500	16 520	69 500	15 620	8 500	9 000	0.5	1.0	59.5	2.34	81.5	3.21
211 EC	55	2.1654	100	3.9370	21	0.8268	96 500	21 690	95 000	21 350	7 500	8 000	0.7	1.4	66.0	2.60	90.0	3.54
212 EC	60	2.3622	110	4.3307	22	0.8661	108 000	24 270	102 000	22 920	6 700	7 500	0.8	1.7	72.0	2.83	100.0	3.94
213 EC	65	2.5591	120	4.7244	23	0.9055	122 000	27 420	118 000	26 520	6 300	6 700	1.0	2.2	78.5	3.09	108.5	4.27
214 EC	70	2.7559	125	4.9213	24	0.9449	137 000	30 790	137 000	30 790	6 000	6 300	1.1	2.5	83.5	3.29	113.5	4.47
215 EC	75	2.9528	130	5.1181	25	0.9843	150 000	33 710	156 000	35 060	5 600	6 000	1.2	2.7	88.5	3.48	118.5	4.67
216 EC	80	3.1496	140	5.5118	26	1.0236	160 000	35 960	166 000	37 300	5 300	5 600	1.5	3.4	95.3	3.75	127.3	5.01
217 EC	85	3.3465	150	5.9055	28	1.1024	190 000	42 700	200 000	44 940	4 800	5 300	1.9	4.1	100.5	3.96	136.5	5.37
218 EC	90	3.5433	160	6.2992	30	1.1811	208 000	46 740	220 000	49 440	4 500	5 000	2.3	5.0	107.0	4.21	145.0	5.71
219 EC	95	3.7402	170	6.6929	32	1.2598	255 000	57 300	265 000	59 600	4 300	4 800	2.8	6.2	112.5	4.43	154.5	6.08
220 EC	100	3.9370	180	7.0866	34	1.3386	285 000	64 000	305 000	68 500	4 000	4 500	3.4	7.4	119.0	4.69	163.0	6.42
221 EC	105	4.1339	190	7.4803	36	1.4173	300 000	67 400	315 000	70 800	3 800	4 300	3.9	8.5	125.0	4.92	173.0	6.81
222 EC	110	4.3307	200	7.8740	38	1.4961	335 000	75 300	365 000	82 000	3 600	4 000	4.7	10.4	132.5	5.22	180.5	7.11
224 EC	120	4.7244	215	8.4646	40	1.5748	390 000	87 600	430 000	96 600	3 400	3 600	5.7	12.6	143.5	5.65	195.5	7.70
226 EC	130	5.1181	230	9.0551	40	1.5748	415 000	93 300	455 000	102 200	3 200	3 400	6.4	14.2	153.5	6.04	209.5	8.25
228 EC	140	5.5118	250	9.8425	42	1.6535	450 000	101 100	510 000	114 600	2 800	3 200	8.5	18.6	169.0	6.65	225.0	8.86
230 EC	150	5.9055	270	10.6299	45	1.7717	510 000	114 600	600 000	134 800	2 600	2 800	10.7	23.6	182.0	7.17	242.0	9.53
232 EC	160	6.2992	290	11.4173	48	1.8898	585 000	131 500	680 000	152 800	2 400	2 600	14.2	31.3	195.0	7.68	259.0	10.20
234 EC	170	6.6929	310	12.2047	52	2.0472	695 000	156 200	815 000	183 100	2 200	3 800	17.3	38.2	207.0	8.15	279.0	10.98
236 EC	180	7.0866	320	12.5984	52	2.0472	720 000	161 800	850 000	191 000	2 200	3 600	18.5	40.7	217.0	8.54	289.0	11.38
238 EC	190	7.4803	340	13.3858	55	2.1654	800 000	179 800	965 000	216 900	2 000	3 400	22.2	48.9	230.0	9.06	306.0	12.05
240 EC	200	7.8740	360	14.1732	58	2.2835	880 000	197 800	1 060 000	238 200	1 900	3 200	26.5	58.5	243.0	9.57	323.0	12.72
244 EC	220	8.6614	400	15.7480	65	2.5591	1 059 999	238 200	1 290 000	289 900	1 700	3 000	36.8	81.0	268.0	10.55	358.0	14.09

Table 1. Specifications of spherical thrust roller bearings

4 Gear System Analysis

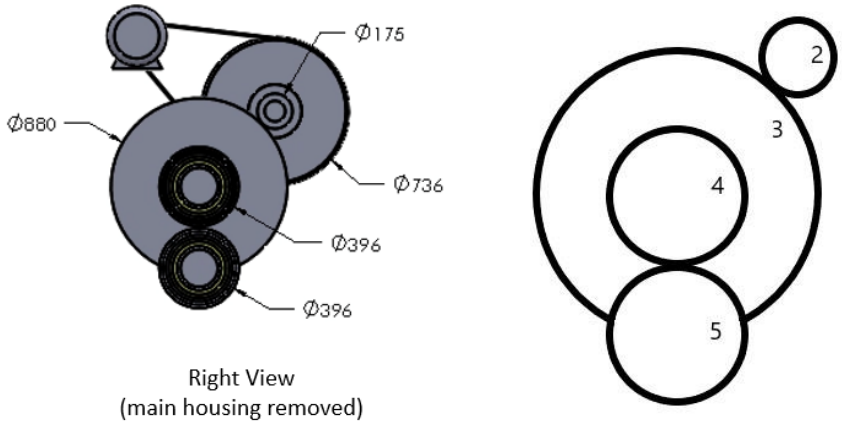

Figure 10. Gear System and Identification

The roll forging machine has a gear system that allows the rollers to rotate at a constant rate. *Figure 10* shows the gear system from the right of the machine with its housing removed. Beside the figure of the gear system a redrawn version is shown that highlights the gears that are

being analyzed. There are four gears identified, starting from gear 2. Gear 3 is a compound gear that is driven by gear 2, and gear 4 is attached to gear 3. Gear 5 is driven by gear 4.

In order to tabulate the speed, torque, and power of the gears, we must first make assumptions about the gears. Gear 2 meshes with the compound gear, but since it can be simplified to the motor input, otherwise what drives the gear system in the first place, gear 2 can be ignored in finding speed, torque, and power. Excluding gear 2 leaves only gear 3, 4, and 5. The rotations per minute and peak torque are given for the roller, and since the rollers are connected to gears 4 and 5, those gears will rotate at the same speed and experience the same peak torque. We decided to use peak torque in the calculations since the torque will rarely exceed the peak torque which ensures that the gears will rarely fail. Once we have an understanding of how the gears work, we can apply the proper gear proportions to find the related speed, torque, and power for each gear. Proportions such as:

$$V = r\omega$$

The above related the velocity of the gears to the radius and the angular velocity or in our case the rotations per minute. Another proportion that related torque in the gears:

$$T = rw_t$$

The torque equation relates the transmitted load and the radius. During calculations, we assumed that the transmitted load experienced by all gears is the same allowing, the torque to vary based on the radius of the gear. Below is a table that compiles the speed, torque and power of the relevant gears.

To find the overall train value of the gear system, all gears were considered including gear 2. The train value was found to be .455 by using the ratio of the speed of the gears that drove over gears that were driven. Since gears 4 and 5 have the same speed, they will cancel out.

$$e = (n_5/n_4)(n_3/n_2)$$
$$e = (65.828/30) = .455$$

Gears	Speed	Torque	Power
Pinion	30 [RPM]	27.5 [kN*m]	825 [kW]
Compound	65.828 [RPM]	58.895 [kN*m]	3876.94 [kW]

Table 1. Speed, Torque, and Power of each gear

As shown in the table above, the power generated by the smaller gear is less than that of the larger gear. We want to perform an in-depth analysis on the wear and fatigue potential for the gear that experiences the greatest stress. Using the oversimplified approach for wear and bending for gears, we can determine which gear experiences the greatest stress, and thus evaluate failure that is significant for the specific gear.

In order to even use the oversimplified approach, assumptions need to be made about the number of teeth for the gears. Assuming that spur gears are commonly used for processes such as longitudinal roll forging, we can assume that the pressure angle will be 20 degrees. Assuming that circular pitch is equal to the circumference of the gear divided by the number of teeth, we can rewrite this to find the number of teeth. We can use similar proportions to find speeds to find the number of teeth for smaller and larger gears. The calculated number of teeth for the pinions was 18 teeth, and for the compound gear it was 40 teeth.

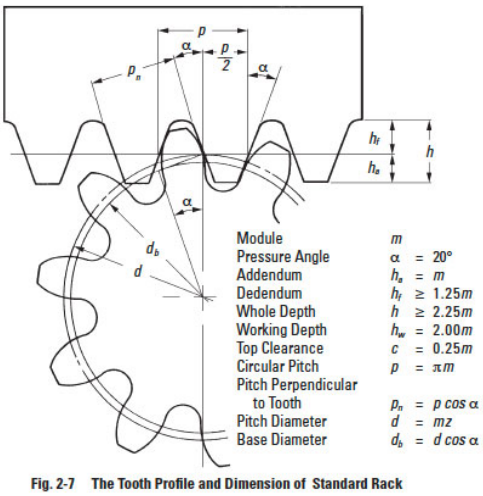

Figure 11. Figure of Tooth Profile for a Gear

Now we can move on to solving the wear and bending failure for each gear. To do this we will use the AGMA approach and apply it to each gear. We will find the allowed stress for each gear, calculate the transmitted load, and then the horsepower generated by each gear depending on the failure criteria. The gear that generates the least amount of horsepower is the gear of most concern.

$$\sigma_b^{allow} = \frac{S_T Y_N}{S_F K_T K_R} \qquad \sigma_c^{allow} = \frac{S_C}{S_H}\frac{Z_N C_H}{K_T K_R}$$

S_T	bending stress number	S_C	surface endurance strength number
Y_N	stress cycle factor	Z_N	stress cycle life factor
S_F	bending fatigue factor	C_H	hardness ratio
K_T	temperature factor	S_H	pitting contact SF
K_R	reliability factor	K_T	temperature factor (as before)
		K_R	reliability factor (as before)

Figure 12. AGMA formulas for allowable stress

We need to make some additional assumptions in order to use AGMA. Face width (*F)* for spur gears is assumed to be a reasonable value between the range of 3 times the pitch diameter and 5 times the pitch diameter. We are assuming a Face width of 4 times the pitch diameter for the pinion gears and the compound gear.

$$F(pinion) = 4 * 396 * 10^{-3} = .069\, m$$

$$F(pinion) = 4 * 880 * 10^{-3} = .1536\, m$$

Modulo (m) should be the same for both gears, in order for them to mesh, and it can be calculated by dividing the diameter of the gear by the number of teeth, $m = .022$.

The velocity (c) of the gears can be calculated using the (η) rpm tabulated above and the ($d,\ D_p, P_d$) diameter of the respective gear.

$$V(pinion) = \pi d\eta \div 60 \text{ s/m} = (\pi(396 * 10^{-3})(30\, RPM) \div 60 = .62\, m/s$$

$$V(compound) = \pi d\eta \div 60 \text{ s/m} = (\pi(880 * 10^{-3})(65.828\, RPM) \div 60$$

$= 3.03\ m/s$

For the elastic coefficient for the wear approach, it was assumed that both gears would be of steel material since this is common for roll forging machines, so (C_p) is assumed to = 191 MPa using the table below from *Shigley's*.

Elastic Coefficient C_p (Z_E), $\sqrt{\text{psi}}$ ($\sqrt{\text{MPa}}$) *Source: AGMA 218.01*

Pinion Material	Pinion Modulus of Elasticity E_P psi (MPa)*	Gear Material and Modulus of Elasticity E_G, lbf/in² (MPa)*: Steel 30×10^6 (2×10^5)	Malleable Iron 25×10^6 (1.7×10^5)	Nodular Iron 24×10^6 (1.7×10^5)	Cast Iron 22×10^6 (1.5×10^5)	Aluminum Bronze 17.5×10^6 (1.2×10^5)	Tin Bronze 16×10^6 (1.1×10^5)
Steel	30×10^6 (2×10^5)	2300 (191)	2180 (181)	2160 (179)	2100 (174)	1950 (162)	1900 (158)
Malleable iron	25×10^6 (1.7×10^5)	2180 (181)	2090 (174)	2070 (172)	2020 (168)	1900 (158)	1850 (154)
Nodular iron	24×10^6 (1.7×10^5)	2160 (179)	2070 (172)	2050 (170)	2000 (166)	1880 (156)	1830 (152)
Cast iron	22×10^6 (1.5×10^5)	2100 (174)	2020 (168)	2000 (166)	1960 (163)	1850 (154)	1800 (149)
Aluminum bronze	17.5×10^6 (1.2×10^5)	1950 (162)	1900 (158)	1880 (156)	1850 (154)	1750 (145)	1700 (141)
Tin bronze	16×10^6 (1.1×10^5)	1900 (158)	1850 (154)	1830 (152)	1800 (149)	1700 (141)	1650 (137)

Figure 13. Table from Shigley's for determining the Elastic coefficient.

For Brinell hardness, we assumed that so long as it's under 400, since that isn't recommended for producing spur gears, and above the Brinell hardness of the material is 197, we chose a reasonable 350 as our Brinell hardness.

Since spur gears are used in the mechanism as pinion and compound gear, and that the material is steel, we chose a reliability factor of ($K_R = .99$).

For selecting the value for stress number for both bending and wear, grade 1 was the acceptable line to use because we don't expect the gears to be doing incredibly precise processes aside from rotating the rollers. S_t for bending was calculated using the Brinell hardness and the respective equation for Grade 1. The same process was applied for calculating S_c for wear.

$$S_t = .533H_b + 833\,MPa = .533(350) + 833\,MPa = 274.85MPa$$

$$S_c = 2.22H_b + 200\,MPa = 2.22(350) + 200MPa = 977\,MPa$$

Y_N, stress cycle factor, and Z_N stress life cycle factor can all be calculated using *N,* the number of cycles, and the figures shown below from *Shigley's.* Formulas based on the Brinell hardness and number of cycles can be used to find the factors.

Figure 14–14

Repeatedly applied bending strength stress-cycle factor Y_N. *(ANSI/AGMA 2001-D04.)*

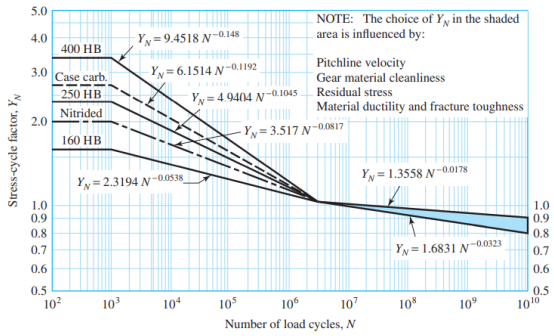

Figure 14–15

Pitting resistance stress-cycle factor Z_N. *(ANSI/AGMA 2001-D04.)*

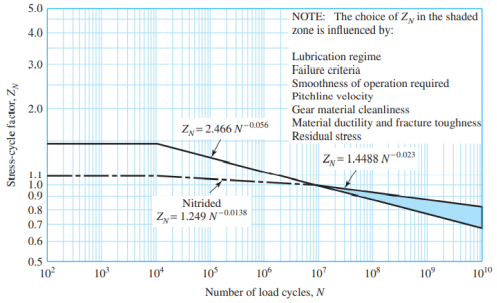

Figure 14. Table from Shigley's for determining Y_N, stress cycle factor, and Z_N stress life cycle factor

$$Y_N = 6.151N^{-.1192} = 6.151(3.744 * 10^6)^{-.1192} = 1.01$$

$$Z_N = 2.466N^{-.056} = (2.466)(3.744 * 10^6)^{-.056} = 1.057$$

For both bending and wear, for both gears we assumed that an additional safety factor wasn't needed to account for failure, so $S_F = S_H = 1$. Since the material temperature exceeds the values in the figure shown below taken from *Stock Drive Products*, we assumed $K_T = .1$

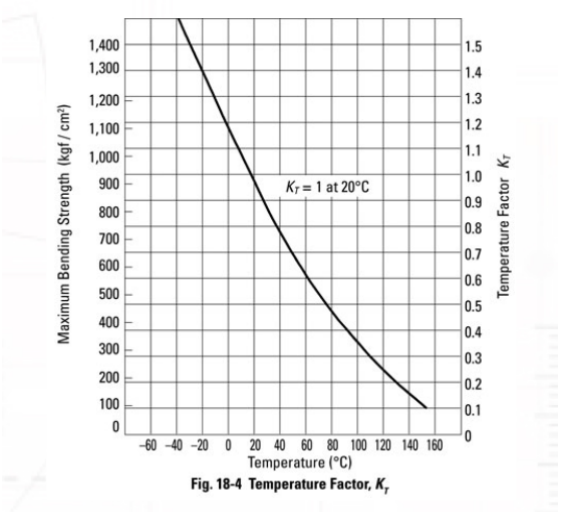

Figure 15. Table from Stock Drive Products for determining the temperature factor K_T

For the pinion gear, the hardness ratio factor is assumed as $C_H = .1$ based on *Shigley's* and since we've assumed the same Brinell Hardness for the compound gear also, the same hardness ratio factor can be applied to it also.

Now we can calculate the allowable wear and bending stress for the compound gear and for both pinion gears.

$$\sigma_b^{allow} = S_T Y_N \div S_F K_T K_R = (274.85MPa)(1.01) \div (1)(.1)(1) = 2775.99\ MPa$$

$$\sigma_C^{allow} = S_C Z_N C_H \div S_H K_T K_R = (977\ MPa)(1.056)(1) \div (1)(.1)(1) = 10317.12\ MPa$$

With the allowable stress values calculated, we can now move on to finding the transmitted load using the formulas shown below.

$$W^t = \frac{\sigma_b^{allow}}{K_o K_v K_s} \frac{F}{p_d} \frac{J}{K_m K_B}$$

$$W^t = \left[\frac{\sigma_c^{allow}}{C_p} \right]^2 \frac{F D_p I}{K_o K_v K_s K_m C_F}$$

GIVEN

SAME

Figure 16. Formulas from Shigley's for calculating the transmitted load for bending and wear of gear

We need to make additional assumptions about unknown factors in order to find the transmitted loads.

The overload factor, K_o, was assumed to be = 1.75 based on the table below from *Shigley's.* The machine will generate moderate shock due to the preforming of the dies onto the material, in addition to the medium shock from the motor that powers the gears.

Table of Overload Factors, K_o

	Driven Machine		
Power source	Uniform	Moderate shock	Heavy shock
Uniform	1.00	1.25	1.75
Light shock	1.25	1.50	2.00
Medium shock	1.50	1.75	2.25

Figure 17. Table from Shigley's for Overload Factor K_o

The geometry factor J was determined using the figure below from *Shigley's.* The pinion gear would be an 18 teeth gear driving the 40 teeth gear, $J(pinion) = .32$. The compound gear would be a 40 teeth gear driving the 18 teeth gear, $J(compound) = .33$.

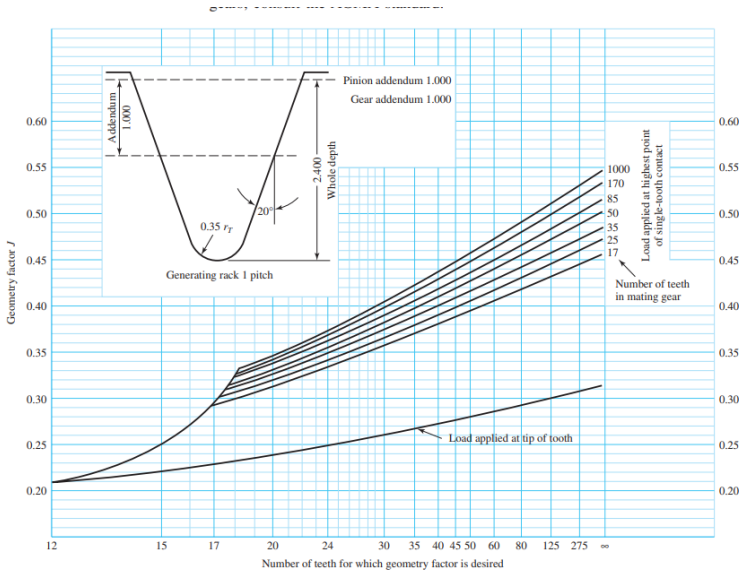

Figure 18. Table from Shigley's for Geometry Factor J

The pitting resistance geometry factor *I* was found using the formulas below for internal gears, where $m_G(speed\ ratio) = d_{compound} \div d_{pinion} = 2.2$ *and* $\phi_t = 20\ degrees.$

$$I = \begin{cases} \dfrac{\cos\phi_t \sin\phi_t}{2m_N} \dfrac{m_G}{m_G + 1} & \text{external gears} \\ \dfrac{\cos\phi_t \sin\phi_t}{2m_N} \dfrac{m_G}{m_G - 1} & \text{internal gears} \end{cases}$$

Figure 19. Formula from Shigley's for Pitting Resistance Geometry Factor I

$$I = [cos(20)sin(20) \div 2(2.2)] \times [2.2 \div (2.2 - 1)] = .13$$

The size factor K_s was assumed to be equivalent to 1 according to *Shigley's* because we assumed the gears had no nonuniformity relating to tooth size, the diameter of the part, face width, and additional factors mentioned in *Shigley's.*

The load distribution factor K_m *and* K_H was assumed to be 1 based on *Shigley's* as we can't use it since the face widths *F* of both gears is less than 40 inches.

The rim thickness factor K_b was assumed to be 1 *based on Shigley's* since the rim thickness of the gears we felt was sufficient for the longitudinal roll forging process.

The surface condition factor C_F was assumed to be 1 based on *Shigley's* since that is the specification for spur gears.

The dynamic factor K_V is calculated using the formulas below from *Shigley's*. Q_v is assumed to be equal to 9, as we have assumed that the gears are produced on a machining mill, thus are of fairly precise quality.

$$K_v = \begin{cases} \left(\dfrac{A + \sqrt{V}}{A}\right)^B & V \text{ in ft/min} \\ \left(\dfrac{A + \sqrt{200V}}{A}\right)^B & V \text{ in m/s} \end{cases}$$

$$A = 50 + 56(1 - B)$$
$$B = 0.25(12 - Q_v)^{2/3}$$

Figure 20. Formula from Shigley's for Dynamic Factor

$$K_V = [(A + \sqrt{200V}) \div A]^B$$

$$B = .25\,(12 - Q_v)^{2/3} = .25\,(12 - 9)^{2/3} = .52$$

A = 50 + 56(1-B) = 50 - 56(1-.52) = 76.88

$$K_V(pinion) = [(A + \sqrt{200V}) \div A]^B = [(76.88 + \sqrt{200 * .62}) \div 76.88]^{.52} = 1.07$$

$$K_V(compound) = [(A + \sqrt{200V}) \div A]^B = [76.88 + \sqrt{200 * 3.03} \div 76.88]^{.52} = 5.2$$

Using these factors identified we can now calculate the transmitted load for the pinion gear and the compound gear.

$$W^t(pinion\ bending) = \sigma_b^{allow} F J \div K_o K_V K_s P_d K_m K_b$$

$$= (2775.99\ MPa)(.069)(.32) \div (1.75)(1.07)(1)(.396)(1)(1) = 82\ MN$$

$$W^t(compound\ bending) = \sigma_b^{allow} F J \div K_o K_V K_s P_d K_m K_b$$

$$= (2775.99\ MPa)(.1536)(.33) \div (1.75)(5.2)(1)(.88)(1)(1) = 17\ MN$$

$$W^t(pinion\ wear) = [\sigma_c^{allow} \div C_p]^2 F D_p I \div K_o K_V K_s K_m C_F$$

$$= [(10317.12\ MPa) \div (191\ MPa)]^2 (.069)(.396)(.13) \div (1.75)(1.07)(1)(1)(1)$$

$$= 5.53\ \text{N}$$

$$W^t(compound\ wear) = [\sigma_c^{allow} \div C_p]^2 F D_p I \div K_o K_V K_s K_m C_F$$

$$= [(10317.12\ MPa) \div (191\ MPa)]^2 (.1536)(.88)(.13) \div (1.75)(5.2)(1)(1)(1)$$

$$= 5.6\ \text{N}$$

Now we can use the transmitted load, and compare the power transmission generated by the gears to see which gear is limiting in the mechanism.

$$H = W^t V / 33000$$

$$H(pinion\ bending) = W^t V / 33000 = (82\ MN)(.62)/33000 = 1540.6\ HP$$

$$H(compound\ bending) = W^t V / 33000 = (17\ MN)(3.03)/33000 = 1560\ HP$$

$$H(pinion\ wear) = W^t V / 33000 = (5.53N)(.62)/33000 = 1.03 * 10^{-4}\ HP$$

$$H(compound\ wear) = W^t V / 33000 = (5.6N)(3.03)/33000 = 5.14 * 10^{-4}\ HP$$

Based on this, it can be concluded that the pinion gear is the limiting gear in the mechanism and the failure mode is wear stress. This makes sense as we would expect the gears directly in line with the rollers to experience the greatest amount of stress in the machine. However transmitted load calculated for both gears exceeds the max radial force that the rollers

generate based on assumptions. Realistically this conclusion seems unlikely. It is possible that an overly conservative estimation of torque was made for the assumptions of the gear mechanism.

5 Conclusion

This report details the design of a roll forging machine's bearings, rollers, and gear system. For each component of the machine, assumptions and calculations were made. For the rollers, deflection was found analytically through tables A-9 and backed by FEA results. The reaction forces at the bearings were also found by balancing the forces on the rollers in both the x-y and x-z plane. Additionally, fatigue and static failure factor of safeties were analyzed for the rollers. Bearing specifications were selected and catalog life rating was found. Gear analysis included but was not limited to specifications of speed, torque, and power of each gear through proper gear relations of torque and velocity. Finally gear wear and fatigue was analyzed using an oversimplified approach. We are comparing our results with the material properties of the material undergoing the roll forging process and Alloy Steel. To improve the machine and minimize the chance of failure, the components can be strengthened either by using a stronger material or increasing the size of the part itself.

Work Cited

Budynas, Richard Gordon, and J. Keith Nisbett. *Shigley's Mechanical Engineering Design*. McGraw-Hill Education, 2015.

"Calculation of Loads: Basic Bearing Knowledge: Koyo Bearings /JTEKT Corporation." *Basic Bearing Knowledge | Koyo Bearings /JTEKT CORPORATION*, https://koyo.jtekt.co.jp/en/support/bearing-knowledge/5-3000.html.

Designing with Plastic Gears and General Considerations of Plastic Gearing, https://sdp-si.com/plastic/design-of-plastic-gears.php.

SKF Bearings and Mounted Products. SKF.

Zahalka, Martin, et al. "Cross Wedge Rolling and Forging Rolls as Additional Devices in Closed Die Forging." *DAAAM Proceedings*, 2016, pp. 0530–0535., https://doi.org/10.2507/26th.daaam.proceedings.072.

"440c." *Wikipedia*, Wikimedia Foundation, 30 July 2021, https://en.wikipedia.org/wiki/440C#:~:text=It%20is%20a%20bearing%20steel,quenched%20to%20achieve%20maximum%20hardness.